

Composite scaffolds based on bacterial cellulose for wound dressing application

Citation

DAS, Munmi, Oyunchimeg ZANDRAA, Chethana MUDENUR, Nabanita SAHA, Petr SÁHA, Bishnupada MANDAL, and Vimal KATIYAR. Composite scaffolds based on bacterial cellulose for wound dressing application. *ACS Applied Bio Materials* [online]. vol. 5, iss. 8, American Chemical Society, 2022, p. 3722 - 3733 [cit. 2023-11-24]. ISSN 2576-6422. Available at <https://pubs.acs.org/doi/10.1021/acsabm.2c00226>

DOI

<https://doi.org/10.1021/acsabm.2c00226>

Permanent link

<https://publikace.k.utb.cz/handle/10563/1011081>

This document is the Accepted Manuscript version of the article that can be shared via institutional repository.

Composite Scaffolds Based on Bacterial Cellulose for Wound Dressing Application

Munmi Das, Oyunchimeg Zandraa, Chethana Mudenur, Nabanita Saha, Petr Sába, Bishnupada Mandal, and Vimal Katiyar*

Munmi Das — Department of Chemical Engineering, Indian Institute of Technology, Guwahati, Assam 781039, India; orcid.org/0000-0003-4388-8815

Oyunchimeg Zandraa — Centre of Polymer Systems, University Institute, Tomas Bata University in Zlín, 760 01 Zlín, Czech Republic

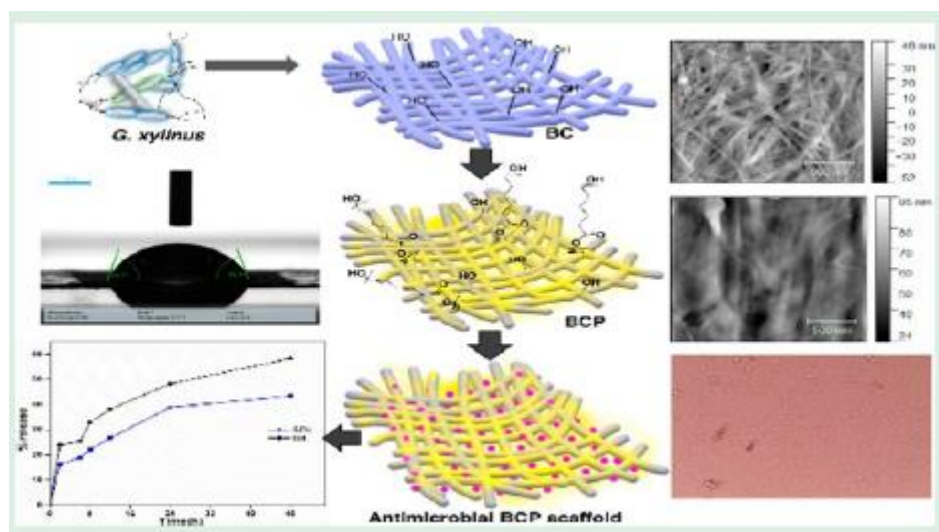
Chethana Mudenur — Department of Chemical Engineering, Indian Institute of Technology, Guwahati, Assam 781039, India; orcid.org/0000-0002-1149-4742

Nabanita Saha — Centre of Polymer Systems, University Institute, Tomas Bata University in Zlín, 760 01 Zlín, Czech Republic

Petr Sába — Centre of Polymer Systems, University Institute, Tomas Bata University in Zlín, 760 01 Zlín, Czech Republic

Bishnupada Mandal — Department of Chemical Engineering, Indian Institute of Technology, Guwahati, Assam 781039, India

Vimal Katiyar — Department of Chemical Engineering, Indian Institute of Technology, Guwahati, Assam 781039, India; orcid.org/0000-0003-4750-7653; Email: vkatiyar@iitg.ac.in



ABSTRACT

Wound dressing materials fabricated using biocompatible polymers have become quite relevant in medical applications, and one such material is bacterial cellulose (BC) with exceptional properties in terms of biocompatibility, high purity, crystallinity (~88%), and high water holding capacity. However, the lack of antibacterial activity slightly restricts its application as a wound dressing material. In this work, polycaprolactone (PCL) was first impregnated into the BC matrix to fabricate flexible bacterial cellulose-based PCL membranes (BCP), which was further functionalized with antibiotics gentamicin

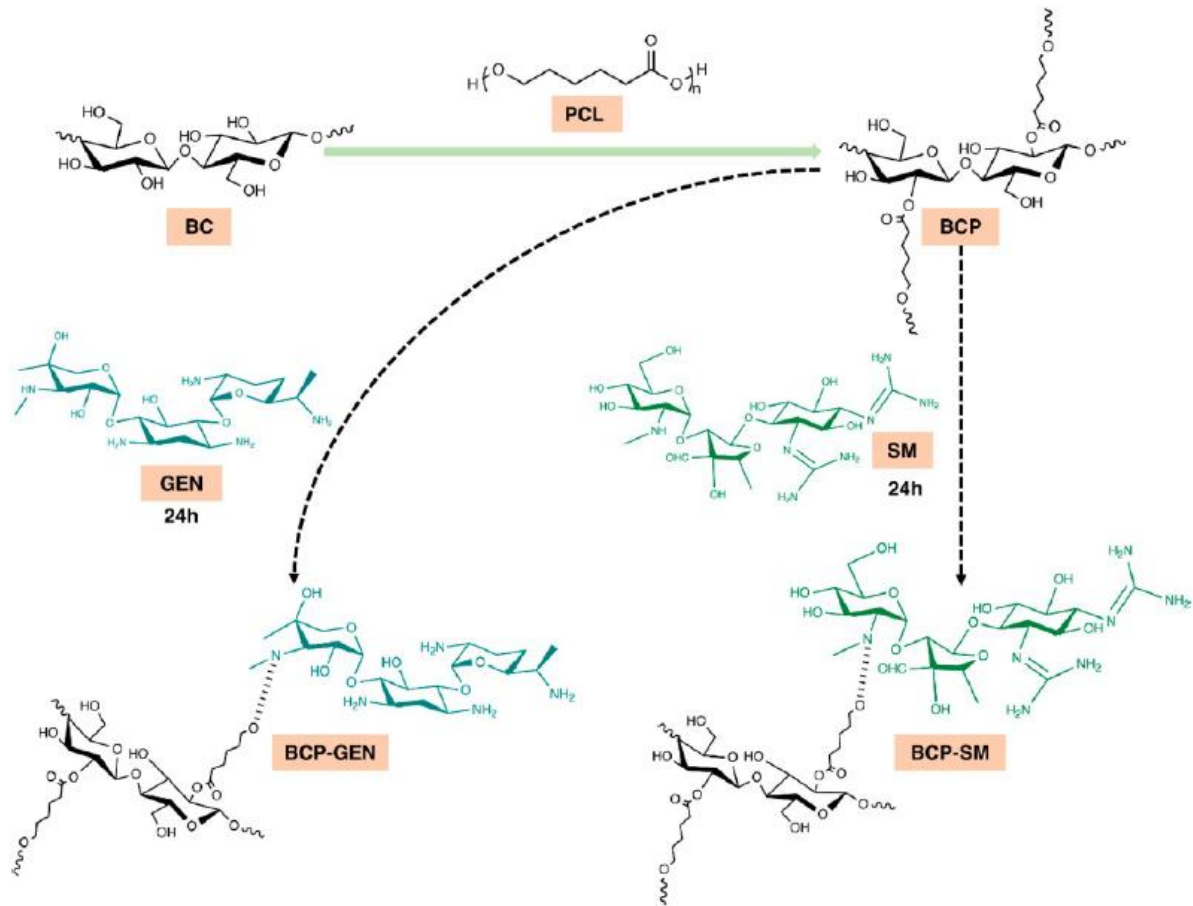
(GEN) and streptomycin (SM) separately, to form wound dressing composite scaffolds to aid infectious wound healing. Fourier transform infrared spectroscopy (FT-IR) results confirmed the presence of characteristic PCL and cellulose peaks in the composite scaffolds at 1720 cm^{-1} , 3400 cm^{-1} , and 2895 cm^{-1} , respectively, explaining the successful interaction of PCL with the BC matrix, which is further corroborated by scanning electron microscopy (SEM) images. X-ray diffraction (XRD) studies revealed the formation of highly crystalline BCP films (~86%). In vitro studies of the BC and BCP scaffolds against baby hamster kidney (BHK-21) cells revealed their cytocompatible nature; also the wettability studies indicated the hydrophilicity of the developed scaffolds, qualifying the main criterion in wound dressing applications. Energy dispersive X-ray analysis (EDX) of the drug loaded scaffolds showed the presence of sulfur in the composites. The prepared scaffolds also exhibited excellent antimicrobial activity against *Escherichia coli* and *Staphylococcus aureus*. The release profiles initially indicated a burst release (6 h) followed by controlled release of GEN (~42%) and SM (~58%) from the prepared scaffolds within 48 h. Hence, these results interpret that the prepared drug-functionalized cellulosic scaffolds have great potential as a wound dressing material in biomedical applications.

KEYWORDS: Bacterial cellulose, polycaprolactone, gentamicin, streptomycin, antimicrobial properties, biocompatibility, wound dressing

1. INTRODUCTION

Skin, the human body's largest organ, plays a substantial role in protecting the body from pathological organisms by acting as a natural barrier, maintaining the body temperature, homeo-statis, and dehydration.¹ However, these characteristics are disturbed whenever there is an injury or wound, leading to the invasion of bacteria through the site of injury. Thus, to repair these tissues, dressing materials are prepared. A proper wound dressing material should impart a moist environment, allow easy transport of gases, inhibit bacterial infections, should be nontoxic, nonallergenic, and promote heat insulation.² In the recent studies, bacterial cellulose (BC) has grabbed attention in the biomedical field due to its highly pure, biocompatible, nontoxic, and highly hydrophilic nature. These captivating properties make it a suitable contender in biomedical applications such as artificial skin, scaffolds, wound dressing materials, dental implants, and also in food packaging and paper industry.³ BC is generally produced from *Acetobacter xylinum*, which is the most efficient BC producer as it can absorb several types of sugars leading to higher yields of cellulose at $\text{pH} \approx 3-7$ and $25-30\text{ }^\circ\text{C}$ temperature in liquid medium. BC is made up of ultrafine fiber network derived from well-arranged three-dimensional (3D) nanofibers, which results in the formation of hydrogel sheets with higher surface area and porosity.^{4,5} As compared to plant-based cellulose, BC fibrils are very much smaller in diameter as well as length (about 100 times) with tailorable properties based on the composition of culture media, carbon source, and also on the producing organism used. BC also has certain promising properties such as high crystallinity (84-90%), high water holding capacity (WHC) of $\sim 106\text{ g water/g sample}$, ability to reform into 3D structure during synthesis, and high water release rate (WRR), of which WRR and WHC are the most essential attributes, directly connected to the biomedical applications of BC as a dressing material.^{4,6-8} Although BC has quite a few unique properties, it also has some limitation such as lack in antibacterial activity, and optical transparency, which limits its use as an effective wound dressing material for highly infectious wounds.⁹ To meet such application standards, BC is functionalized with various organic or inorganic material such as polymers, metal or metal oxides, solid materials, and nanomaterials possessing antimicrobial property via impregnation, either by in situ or ex situ and several other techniques.

Scheme 1. Reaction Mechanism Showing Impregnation of PCL into the BC Membrane, Followed by Surface Functionalization with Gentamicin (GEN) and Streptomycin (SM)



Recently, nanofibrous polymer composites (NFPC) have acquired attention in biomedical applications due to their superior properties such as larger surface-to-volume ratio and flexibility. Examples of materials used along with BC in NFPC preparation for wound dressing applications are silver nanoparticles, graphene oxide, chitosan, and aloe vera.^{2,8-12}

Because of its biocompatibility, controlled degradability, and miscibility with other polymers, polycaprolactone (PCL) has a wide range of application in controlled drug-delivery and tissue engineering as a scaffold material and as a solid plasticizer in soft compostable packaging.^{13,14} The production route of PCL is economical as compared to counterpart aliphatic polyesters; hence, its utilization in the biomedical devices development is highly demanding. PCL is a linear, semicrystalline polymer possessing rubbery character at room temperature and comprises hexanoate repeating units, obtained by ring-opening polymerization (ROP) of ϵ -caprolactone. It is permeable to low molecular compounds at body temperature, and hence, it is an excellent entrant for controlled drug release and widely practiced as a wound dressing material.¹⁵⁻¹⁷

Gentamicin (GEN) is a highly hydrophilic aminoglycoside antibiotic and is often used against a wide range of bacterial infections, such as *P. aeruginosa*, *E. coli*, and *E. aerogenes*, and is also used in the treatment of bone infections caused by *S. aureus* and many others.¹⁸⁻²⁰ Several studies have reported the use of GEN in controlled drug delivery, as for example Rouabhia et al.²¹ prepared gentamicin activated bacterial cellulose dressings containing 3-aminopropyltriethoxysilane (APTES) as

a coupling agent for drug delivery and wound healing applications. Another widely researched aminoglycoside antibiotic is streptomycin (SM), which is also antibacterial and is mainly used in the treatment of serious infections caused by tuberculosis (*Mycobacterium tuberculosis*), plague (*Yersinia pestis*), and avium (*Mycobacterium avium*), and is considered as one of the most effective and safe medicines for human health system as documented by the World Health Organization (WHO).²²⁻²⁴

To date, BC has been utilized as an antimicrobial material; however, the utilization of GEN and SM functionalized BC is to be further explored. It is well-known that BC has abundant hydroxyl groups on its surface, which enables its easy functionalization and interaction with other materials ultimately resulting in beneficial applications. Thus, considering the unique properties of BC and PCL together, in terms of biocompatibility and biodegradability, herein we propose the fabrication of BC-based composite scaffolds by the impregnation of PCL into the BC network structure. The developed scaffolds showed good biocompatibility toward baby hamster kidney fibroblast cells (BHK-21). The composite scaffolds were then functionalized by the incorporation of antibiotics, GEN and SM, separately to form antimicrobial wound dressing material and the resultant scaffolds showed a wide-spectrum of antibacterial inhibition against *E. coli* and *S. aureus* (**Scheme 1**).

2. EXPERIMENTAL SECTION

2.1. Materials

Bacterial strain *Gluconacetobacter xylinus* CCM 3611, used for the production of BC, was purchased and conserved in the Microbiology Laboratory of the Centre of Polymer Systems, Zlin, Czech Republic. Glucose, peptone, agar, yeast extract, anhydrous disodium phosphate, and citric acid were purchased from Sigma-Aldrich (Czech Republic). Poly(ϵ -caprolactone) of $M_n \approx 78$ kDa was laboratory synthesized by a solvent-free polymerization technique under inert atmosphere in the Centre of Excellence for Sustainable Polymers, Dept. of Chemical Engineering, IIT Guwahati, India. In the polymerization process, initially ethylene glycol (>99% purity, initiator) and tin octoate (>99% purity, catalyst) was allowed to stir for sometime followed by the addition of monomer, ϵ -caprolactone (98% purity), and the reaction time and temperature were optimized to achieve the desired molecular weight. The as-synthesized PCL exhibited a density higher than its monomer (~ 1.130 g/cm³) and a maximum intrinsic viscosity 74.0 cm³/g.²⁵ Streptomycin sulfate (SM) and gentamicin sulfate (GEN) salts were purchased from Himedia and Sigma-Aldrich (India), respectively.

2.2. Synthesis and Purification of Bacterial Cellulose

The standard Hestrin and Schramm (H.S.) medium comprising glucose, peptone, yeast extract, anhydrous disodium phosphate, and citric acid was used as the medium for the BC production.²⁶ Bacterial strain *G. xylinum* was cultured in agar plates for 3 days at 28 °C. Briefly, 5 loopfuls of the grown bacteria were collected and inoculated in a tube containing 5 mL of H.S. medium to prepare initial inoculum for BC production and was incubated for 2 days at 28 °C under static condition. This prepared inoculum was then transferred to sets of sterile 250 mL glass bottles filled with 100 mL of H.S. medium each and the culture bottles were then covered with perforated parafilm for aeration incubation at 28 °C for 15 days under static state. Large scale synthesis of BC was also carried out in glass trays (295 X 230 X 210 mm³) containing 4–6 L of medium to obtain BC membranes of larger size (295 mm X 230 mm and 15 μ m height) and wet weight ~ 125 g [**Supporting Information (Figure S4)**]. The H.S. medium used was autoclaved at 121 °C for 20 min before use. The BC pellicles formed on the

surface of the culture vessels were then collected and soaked in distilled water overnight, and then treated twice with 0.5 N NaOH for 30 min at 80 °C followed by washing with distilled water until neutral pH was achieved.

*2.3. Fabrication of Bacterial Cellulose Based Poly(*ε*-caprolactone) Composites*

The previously treated and purified BC pellicles were placed in a beaker, to which 1:1 (weight) ratio of distilled water was added. A fine suspension of BC in water was achieved in 20 min with the use of a hand blender (Powermaxx, BOSCH, 750W). This suspension was then cast on a silicon tray and allowed to air-dry overnight to get a uniform BC membrane. To develop uniform bacterial cellulose based polycaprolactone (BCP) composites, dried BC membranes were first cut (3 X 4 cm²) and incubated in acetone for 24 h. Thereafter, all the acetone soaked samples were immersed in glass vials containing PCL solution in acetone (2 and 3 wt % PCL) [Supporting Information (**Table S1** and **Figure S5**)].²⁷ The impregnation of PCL into the BC membrane was facilitated with the use of a 2D-Benchrocker. After each incubation (48 h, 72 h, and 120 h), the BC membranes immersed in the PCL solution were taken out, washed with acetone to remove the excess polymer, placed in petriplates, and allowed to dry at room temperature.

2.4. Characterization

The surface topography and morphology of the prepared BC and BCP membranes was assessed using atomic force microscope, AFM (Oxford, Model: Cypher) equipped with a silicon cantilever with spring constant of 42 N/m and resonance frequency 320 kHz. The average thickness of the BC and BCP films were calculated as 15 and 23 μm, respectively. The surface and crosssectional morphology of the prepared BC and BCP membranes were characterized using a field emission scanning electron microscope (Nova NanoSEM by FEI, CZ s.r.o, Brno) at 10 000X magnification. Chemical characteristic of the prepared BC, BCP, and drug loaded membranes was studied using Fourier transform infrared (FT-IR) spectroscopy (Nicolet iS5, Thermo Scientific, USA) in attenuated total reflectance (ATR) mode at room temperature in the frequency range of 4000 cm⁻¹ to 400 cm⁻¹ and the X-ray diffraction (XRD) was conducted using a MiniFlex 600 X-ray diffractometer (Rigaku, Japan) with $2\theta = 4-70^\circ$. The thermal behavior of the fabricated membranes was studied in an inert atmosphere of nitrogen at 10 °C/min heating rate using thermogravimetric and derivative thermogravimetric analysis (TGA and DTG Q500 by TA Instruments, USA) in the 25–600 °C temperature range and differential scanning calorimetry (Phoenix DSC 204 F1 NETZSCH, GmbH) in 30–400 °C range. The contact angle of the dried BC and BCP membranes was evaluated using Kruss GMBH DSA25 (Germany), where a sessile drop of water (~2 μL) was placed on the cellulose sample and the change in behavior of the water droplet in contact with the sample was observed as a function of time (0s to 60s) at 25 °C.

2.5. In Vitro Cytotoxicity Assay and Cell Staining

Baby Hamster Kidney fibroblast cells (BHK-21) were cultured in Dulbecco's modified Eagle's Medium (DMEM) (Gibco) supplemented with 10% fetal bovine serum (FBS) (Gibco). The cytotoxicity assay was determined by a colorimetric assay (MTT Assay), where MTT stock solution of 5 mg/mL was prepared in phosphate-buffered saline (PBS), stored at 4 °C. BHK-21 cells, at a density of 2 X 10³ cells/well, were seeded and allowed to grow overnight in a 96-well microplate, at 37 °C in a humidified atmosphere with 5% CO₂. After discarding the media, BC and BCP membranes (6 cm² of area) were UV sterilized for

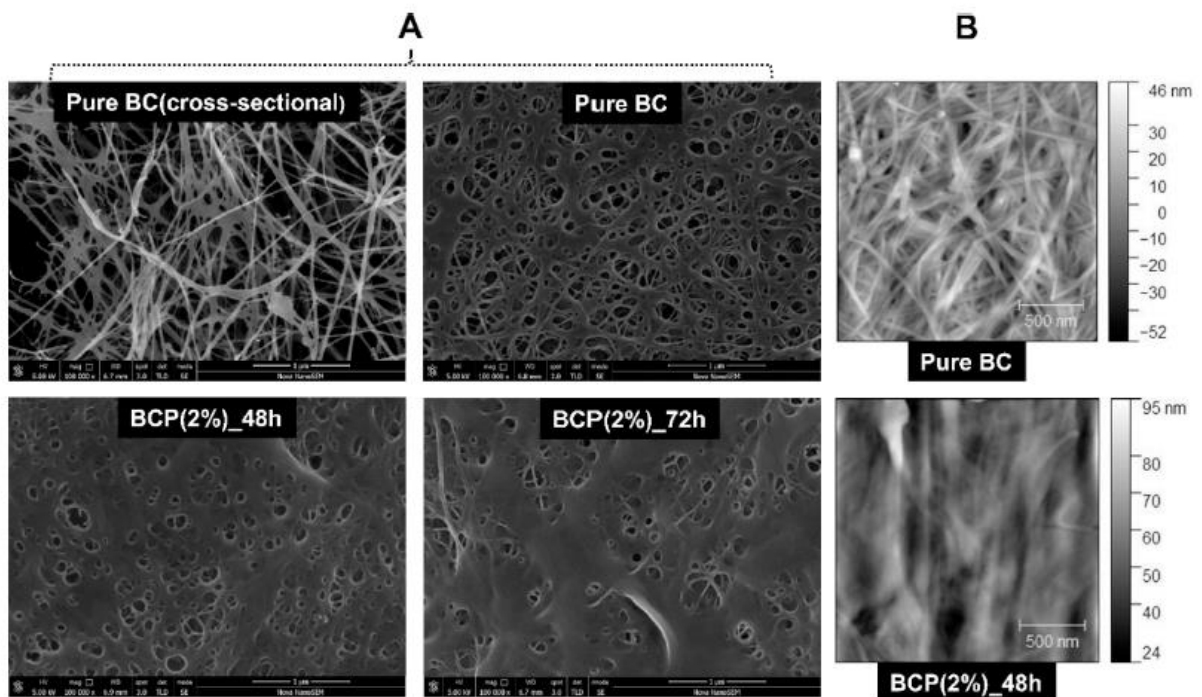
1 h and the extract of the test materials was prepared as per International Standard ISO 10993- 12, and the material surface to extract fluid ratio was kept as 6 cm²/mL. Then the sterilized samples were placed in BHK-21 cell's growth medium for 24 h. After that, the cultures were treated for 24 h, 48 h, and 72 h with the prepared extracted media and the standard culture medium containing only the cells was used as control. After the specific incubation period, all the samples were removed and MTT solution was diluted to 0.5 mg/mL in plain DMEM (without FBS) and the incubation was maintained for further 3 h. Dimethyl sulfoxide (DMSO) was added to each cell well to dissolve the formazan pigment and the absorbance was recorded at 570 nm wavelength using a microplate reader (ELISA). Wells containing only DMSO were considered as blank and the comparison of relative cell viability was calculated in four replicates. The mean values and their standard deviations were calculated, and the graphs were plotted using the closest absorbance values of three replicates out of the four samples.

To study the biocompatibility of the BC and BCP surfaces, the same procedure as above was followed to seed BHK-21 cells in a 96-well plate and circular sample films were cut and placed on it. After specific time (24 h, 48 h, and 72 h), the incubated samples were treated with 4% formaldehyde for 10 min to fix the cells followed by rinsing thrice with PBS. Then DAPI (4',6-diamidino-2-phenylindole) (100 μL) was added to the wells containing the sample and allowed to incubate in dark for 15 min. The cells were then again rinsed with PBS thrice and the images were taken using blue/cyan filter under the fluorescence microscope (Nikon H600L).

2.6. Functionalization of Bacterial Cellulose Films

Two different drug concentration (0.2 and 0.5 mg/mL) of gentamicin and streptomycin, each was prepared in 50 mL of deionized water. The BC and BCP membranes were then immersed in the prepared drug solutions for 24 h at 37 °C in a shaking incubator.

Figure 1. (A) FESEM micrographs of pure BC (cross-sectional and surface view), BCP (2%)_{48h} and BCP (2%)_{72h}. (B) AFM image of pure BC and BCP (2%)_{48h}.



After 24 h, the membranes were taken out and washed with deionized water and dried in room temperature overnight. BC-GEN, BCP- GEN, BC-SM, and BCP-SM are the abbreviations used for GEN-loaded BC, GEN-loaded BCP, SM-loaded BC, and SM-loaded BCP membranes, respectively.

The surface morphology of the drug-loaded BC and BCP scaffolds was analyzed using a field emission scanning electron microscope (ZEISS Sigma, FESEM, USA) at 14 000 X magnification.

Energy dispersive X-ray analysis (EDX) (Zeiss, Gemini) was performed with an aim to identify the chemical compositions of prepared samples in terms of weight percentages (wt %) of elements Carbon (C), oxygen (O), nitrogen (N), and sulfur (S).

2.7. Antimicrobial Assay

Antimicrobial activity of the pure BC, BCP, BC-GEN, BCP- GEN, BC-SM, and BCP-SM samples was determined against *Staphylococcus aureus* and *Escherichia coli*. Luria-Bertani (LB) broth and agar (HiMedia Laboratories) were used for this study. At first, the cultures were inoculated in LB broth and allowed to grow at 37 °C, overnight. Further, the cultures were diluted to get a concentration of 2×10^9 CFU/mL for *E. coli* and 2×10^{10} CFU/mL for *S. aureus*, and used as an inoculum for the antimicrobial assay. Circular discs of each sample were cut in triplicates and UV-sterilized for 1 h before use. The discs were then placed on agar plates containing both the model bacteria separately and allowed to incubate for 24 h at 37 °C, and the zone of inhibition was measured in millimeter from the growth inhibited by the discs. Gentamicin (10 µg) control (Himedia Laboratories) was also placed separately on agar plates containing *E. coli* and *S. aureus* to check the bacterial inhibition [**Supporting Information (Figure S3)**].

2.8. In Vitro Drug Release Study

In vitro release profile of the drug-loaded membranes were carried out by placing 5 mg of each sample (BCP-GEN and BCP-SM) in plastic vials containing 10 mL of phosphate-buffer saline solution (PBS, pH 7.4). These vials were then incubated at 37 °C, and at specific time interval, 3 mL of sample medium was removed and replaced with fresh buffer solution. The cumulative drug release into the PBS solution was measured using an UV-vis spectrometer (Lambda 25, PerkinElmer USA) at wavelengths 232 and 240 nm for GEN and SM, respectively.

3. RESULTS AND DISCUSSION

3.1. Fabrication of BCP Membranes and Their Characterization

This study discusses the property enhancement of bacterial cellulose membranes with the impregnation of PCL into its matrix by incubating the cellulose films in PCL solution. The presence of ester bond in the structure of PCL is expected to react with the abundant hydroxyl groups present on the BC surface resulting in the formation of flexible BCP membranes. These membranes were then functionalized with GEN and SM to produce antimicrobial scaffolds. As both the antibiotics used are aminoglycosides, the amino groups present in their structure react with the hydroxyl groups present in the BCP structure (**Scheme 1**).

The surface morphologies of BC and BCP membranes are shown in **Figure 1A**. Pure BC membrane showed well-defined, closely intertwined, and oriented fibrils with a typical 3dimensional web-like

highly porous network structure, which also confirmed its higher crystallinity.^{16,21} The AFM images (**Figure 1B**) also suggested well-defined fibrillar orientation of BC with long and smooth fibers of diameter in the range of 35-200 nm. The high surface area of the BC matrix allowed the successful impregnation of PCL into its interpenetrating porous structure in the BCP membranes, as observed in **Figure 1A,B**. A smooth and dense morphology is observed for both BCP (2%)_{48h} and BCP (2%)_{72h} membranes, where the polymer layers are present on the surface as well as inside the pores of the BC matrix indicating a good fiber-matrix interaction. The average thickness of each BC bundle was calculated to be ~121 nm in Figure 1B, whereas in case of BCP, the BC bundles were almost covered and filled with PCL, so a few small bundles of average thickness ~54 nm appeared on the surface. The root-mean-square surface roughness value of BC and BCP membranes was estimated to be 3.46 and 5.61 nm, and the height profiles of BC and BCP suggested a maximum height of ± 37 and ± 70 nm, respectively [**Supporting Information (Figure S6)**]. Also it is noteworthy that even after 72 h incubation of the BC mat in PCL solution, some pores are still visible on the surface of BCP membrane, which could further facilitate the cell colonization in the membranes when used as a drug carrier. The surface morphology of the drug loaded BC membranes, BC-GEN, and BC-SM [**Supporting Information (Figure S1)**] further indicated the intact microstructure of BC with the presence of agglomerated drug particles spread over the surface and inside the pores.²⁸

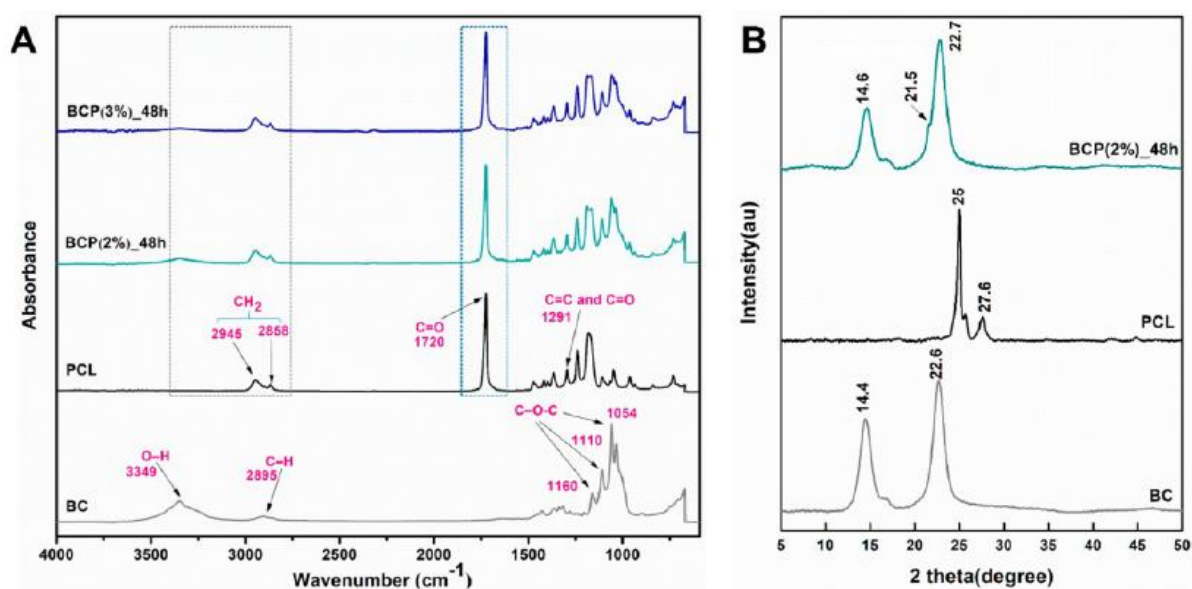


Figure 2. (A) FTIR spectra and (B) XRD plot of BC, PCL, and BCP membranes.

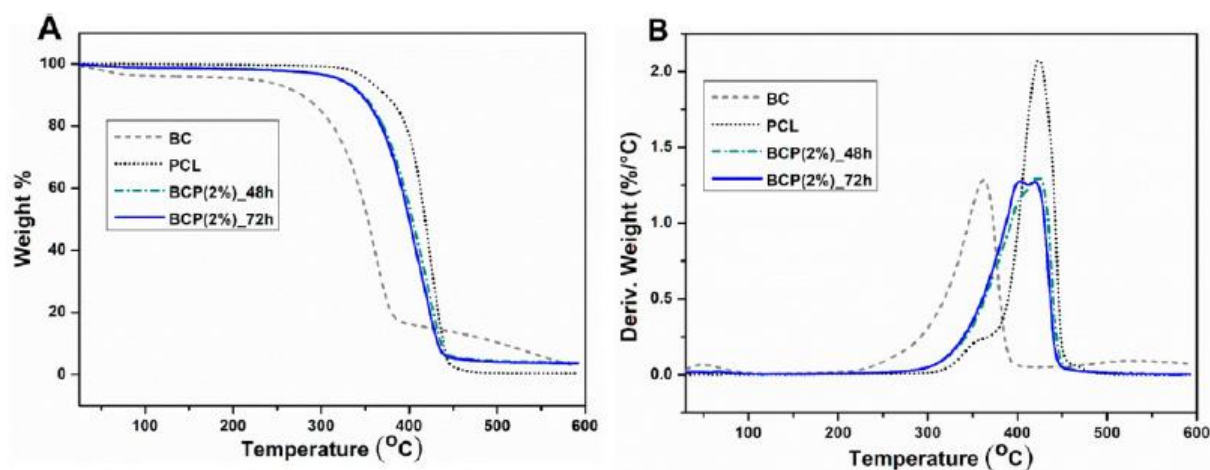


Figure 3. (A) TGA and (B) DTG thermographs of the fabricated BC, PCL, and BCP membranes.

The chemical and physical attributes of the synthesized BC and its composites (BCP) were studied using FT-IR as shown in **Figure 2A**. Pure BC exhibited a strong O—H stretching around 3349 cm^{-1} conforming the intramolecular H-bond, C—H vibration stretching at 2895 cm^{-1} , and the C—O—C stretching vibration is observed around an intense peak at 1054 cm^{-1} .^{29,30} The ~75% crystallinity of PCL could be justified by the presence of C=C and C=O stretching vibration bands at 1291 cm^{-1} . Similarly, a strong C=O stretching band is located at 1720 cm^{-1} , which also refers to the high crystallinity % of PCL. The characteristic symmetric and asymmetric CH_2 stretching was found around 2858 cm^{-1} and 2945 cm^{-1} , respectively.³¹ The BCP membranes showed the presence of the characteristic cellulose and PCL peaks around 3400 and 2895 cm^{-1} related to BC and 2945 , 2858 , and 1720 cm^{-1} from PCL.²⁹ Thus, the interaction between BC and PCL is confirmed, which is also consistent with the change in surface morphology of the prepared composite membranes as shown by SEM images (**Figure 1A**). The crystallinity of the prepared membranes was studied using XRD analysis as shown in **Figure 2B**. Pure BC exhibited a highly crystalline structure, with strong polymeric chain network and slightly lower flexibility.³² Broad diffraction peaks were observed at 16 - 17° and 27° , which indicated the formation of cellulose type I for the pure BC membrane. PCL also exhibited its crystallinity with two diffraction peaks, at around 25 and 27.6 degrees.^{25,33} The presence of cellulose type I peaks in the composite membrane suggests that the BC structure was not disturbed in the composite preparation. The sharp intensity of the peaks indicates highly crystalline nature; however, there is a slight difference in the relative intensity of the peaks, which could be contributed as the change in orientation of the cellulose fibers in interaction with the polymer. Pure BC and PCL revealed a highly crystalline nature (~88% and ~75% crystallinity, respectively). The addition of PCL into the BC network resulted in composites with nearly 84-86% crystallinity exhibiting the same crystalline phase as BC and PCL. The calculation of percentage crystallinity for each membrane is shown in **Table S3 (Supporting Information)**.

From the thermal studies (TGA-DTG) as shown in **Figure 3A,B**, it was observed that the thermal stability of the composites increased significantly with the incorporation of PCL into the BC matrix. Clearly, it was evident that the inherent higher thermal stability of PCL enhanced the thermal property of the final composite membranes. An initial smaller weight loss was observed for BC (~3%) below $150\text{ }^\circ\text{C}$ caused by the evaporation of water from its polysaccharide structure, which is not that prominent in the PCL and BCP membranes.³⁴ The most significant degradation leading to weight and structural change occurred in the 250 - $450\text{ }^\circ\text{C}$ range for all the samples, which is attributable to the degradation of crystalline part and depolymerization of the glycosidic units. The final stage above $500\text{ }^\circ\text{C}$ could be associated with the carbonaceous residue breakdown leading to char oxidation.³⁵ As observed from **Figure 3**, PCL exhibited a maximum weight loss temperature (T_{max}) at $\sim 441\text{ }^\circ\text{C}$, while native BC has a $T_{max} \approx 378\text{ }^\circ\text{C}$. An increase in onset degradation temperature (~ 43 to $54\text{ }^\circ\text{C}$) for the composite samples as compared to BC could be projected as the presence of PCL in its structure. The lower thermal stability of pure BC compared to pure PCL is due to the chemical composition of BC, which comprises of hydroxyl end groups, resulting in the restriction of the chain mobility. All of the samples showed one-step degradation and the initial and maximum degradation temperature along with weight residue of all the samples are compiled in the **Supporting Information (Table S2)**. The ash content of BC and BCP samples was ~4%, whereas PCL almost completely degraded at $600\text{ }^\circ\text{C}$.

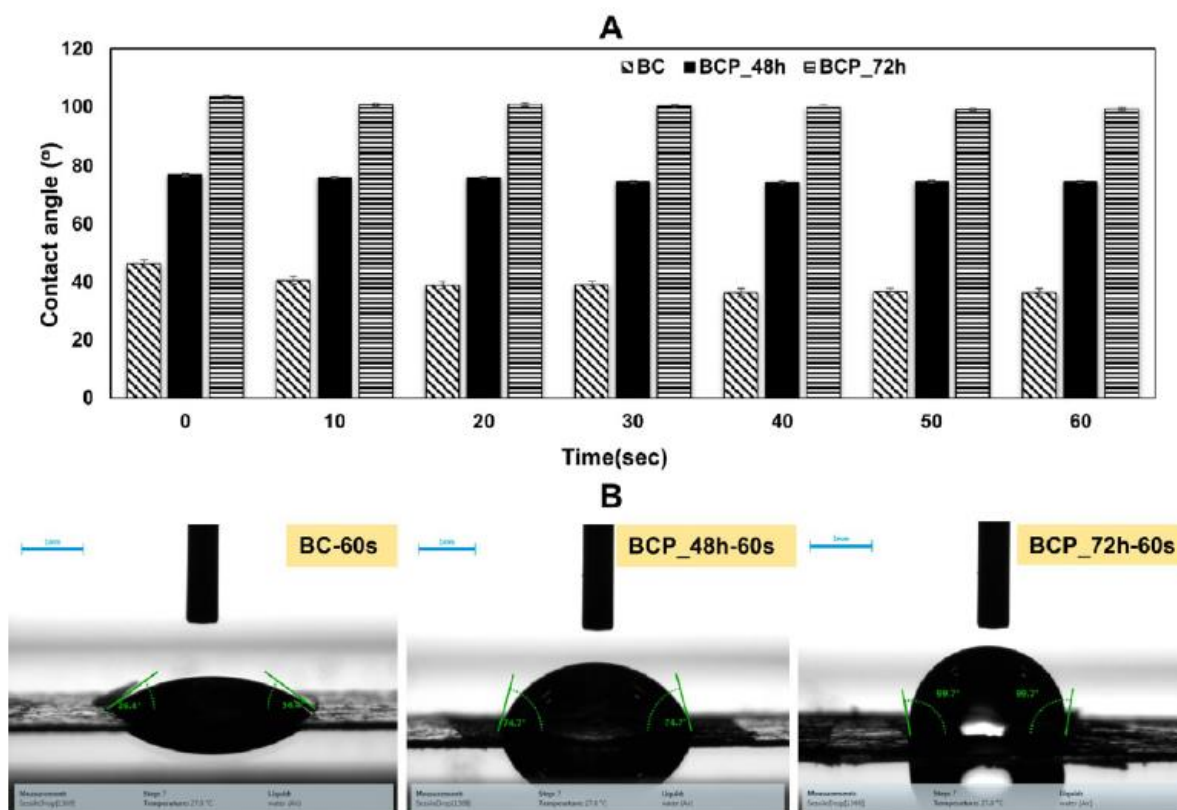


Figure 4. (A) Contact angle measurement of BC, BCP_48h, and BCP_72h membranes over a time period of 0 to 60 s. (B) Images of water contact angles of BC, BCP_48h, and BCP_72h recorded at 60 s.

The thermal transition of BC and the prepared composites was studied using DSC as shown in **Figure S2 (Supporting Information)**, where from 27 to 124 °C, an endothermic event was observed indicating the dehydration of surface water mostly around 70 °C for both BC and BCP membrane. The endothermic events around 348 to 372 °C for both BC and BCP could be attributed to the melting of crystalline regions of respective polymers. This decomposition is also confirmed by the single-step degradation in TGA analysis (**Figure 3**), which overall concludes that the melting phenomenon is followed by degradation for all the samples. The higher thermal stability could also be connected with the highly crystalline and oriented structure of the cellulose matrix and its composites.^{36,37}

Contact angle measurement was carried out to understand the water absorption and hydrophilicity of the developed BC and BCP membranes (**Figures 4A,B**). The high surface energy and the presence of abundant -OH group within and in between the adjacent cellulose structure create an extensive hydrogen bonding (—OH---O-), thereby making BC a highly hydrophilic material. So whenever a water droplet falls on its surface, BC absorbs it immediately, leading to a lower contact angle (~36° in 60 s) as shown in **Figure 4B**. However, as most of the -OH groups present in the surface becomes already occupied, the water contact angle tends to remain constant after a certain time (60 s). The absorption of water droplet onto the surface is also dependent on the porosity of the sample.³⁸ It was observed that the contact angle of BCP samples increased from 74 to 99° (in 60 s) with increase in incubation period of the BC membrane in PCL solution, that is, from 48 to 72 h. As a result, the BCP membranes became resistant to water because of the impregnation of hydrophobic PCL in its surface and network. However, the motive behind the incorporation of PCL into the BC membrane is to produce a stretchable wound dressing material, so BCP membranes incubated for 48 h were used for the antimicrobial and cytotoxicity tests as they have contact angle of ~74°, which is satisfactory for wound

dressing applications.³⁹ The images of the water droplets on the BC and BCP membranes recorded at 60 s time period are shown in **Figure 4B**.

3.2. Antibacterial Activity of Drug-Loaded Films and Their Elemental Composition

The bacterial growth of the pure and drug-loaded films was evaluated with the inoculation of the sample discs in Gram-negative and Gram-positive bacteria, *E. coli* and *S. aureus*. The hydrophilicity associated with BC is an added advantage to be used as a drug carrier system for wound healing applications, as it provides a moist environment and promotes the healing process by enhancing angiogenesis and collagen synthesis, and inhibits bacterial infections.⁴⁰

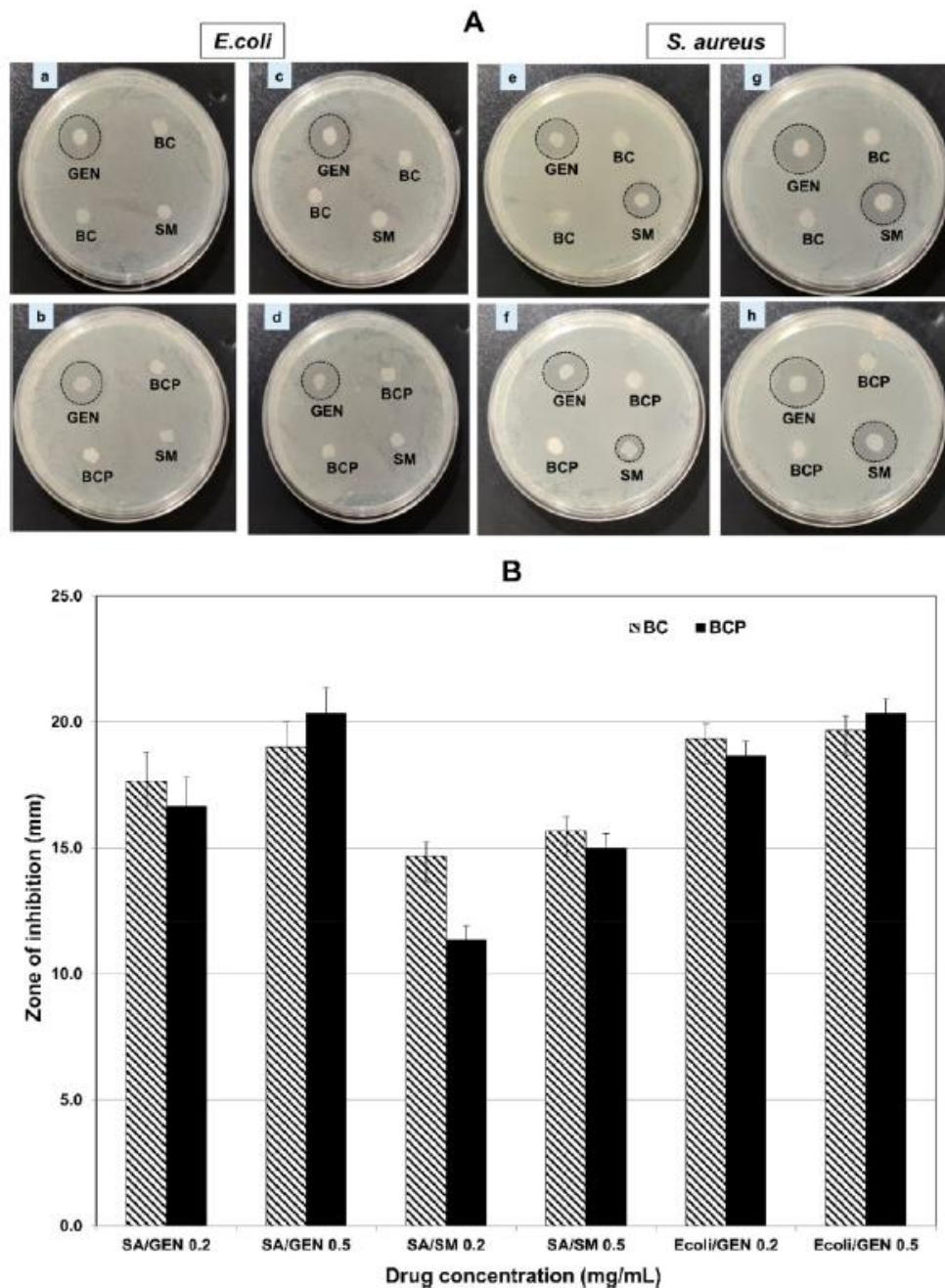


Figure 5. (A) Photographs of gentamicin- and streptomycin-loaded BC and BCP discs showing antibacterial activity against bacteria, *E. coli* and *S. aureus*. (B) Zone of inhibition in millimeters of the drug-loaded films against both the bacteria.

However, pure BC lacks antibacterial characteristics, which is an important aspect in wound dressing applications, with this motive antibiotic-loaded BC and BCP films are being developed in this work. After 24 h of incubation, wider bacterial growth inhibition was evident for the gentamicin- and streptomycin-loaded discs (BC-GEN, BCP-GEN, BC-SM, and BCP-SM) against *S. aureus* (Figure 5A); however, in *E. coli*, only gentamicin-loaded discs exhibited inhibition zone as the bacteria provided resistance to streptomycin due to its genetic encoding.⁴¹ Pure BC and BCP clearly does not have an effect on the bacterial growth, with no inhibition zone observed in Figure 5A. The quantitative evaluation of zone of inhibition exhibited by each sample is shown in Figure 5B.

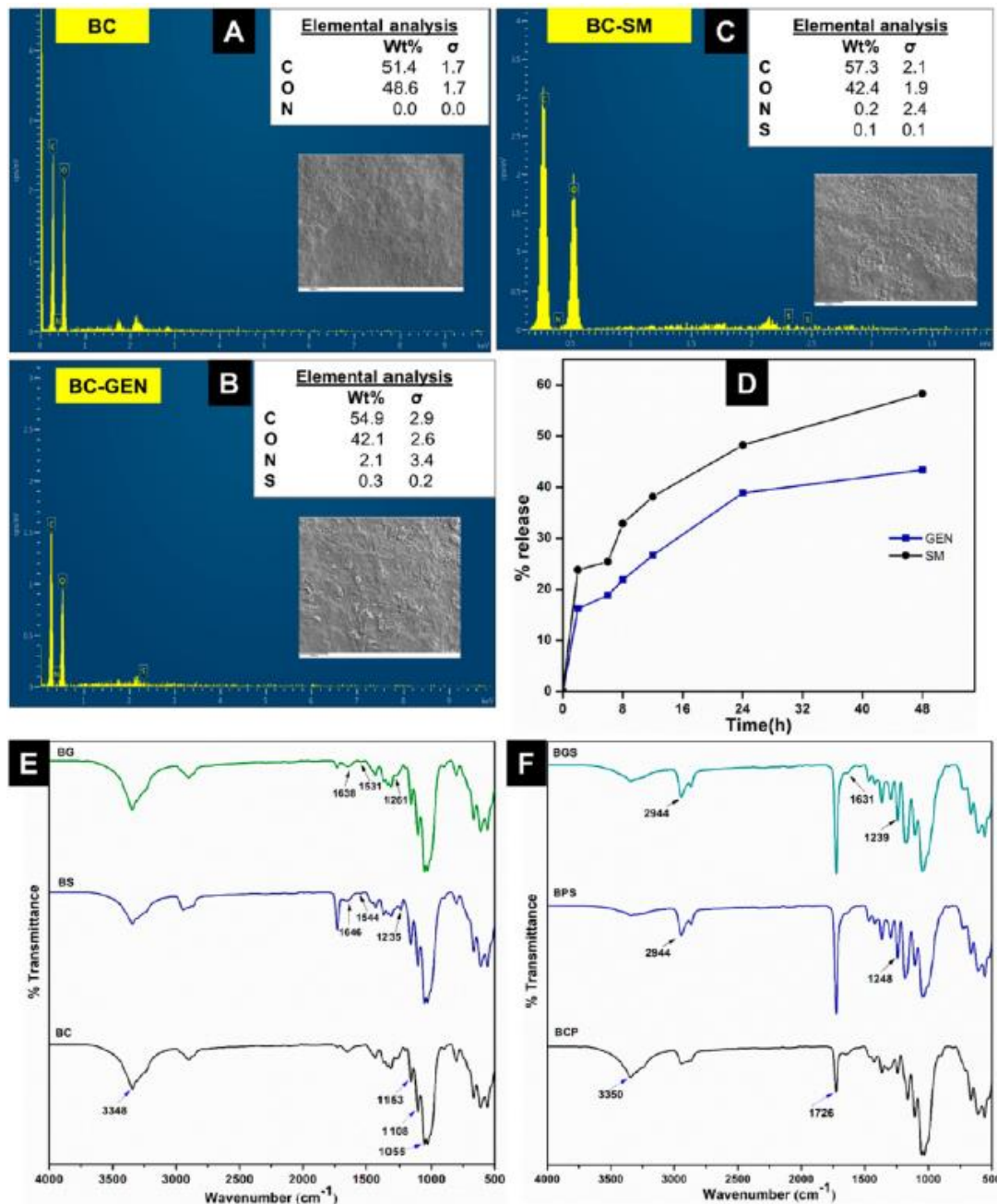


Figure 6. EDX patterns and elemental composition of (A) BC, and drug-loaded BC membranes, (B) BC-GEN and (C) BC-SM. (D) Release behavior from the GEN and SM-loaded BCP films at pH 7.4. (e) FTIR spectra of BC, BS, and BG, and (F) FTIR spectra of BCP, BPS, and BPG.

Both the tested drugs (GEN and SM) showed a concentration-dependent killing activity, which is specific to the drug carrier systems. BC showed a better performance as a drug carrier at a lower dose of ~ 0.2 mg/mL, whereas the BCP samples showed better inhibition at slightly higher doses of ~ 0.5 mg/mL, which is due to the easy penetration of drug into the voids of porous BC matrix as observed from FESEM images (**Figure 1A**). The morphology of the drug-loaded BC membranes (**Figure S1**) indicates the presence of agglomerated drug particles on the BC surface. Gentamicin control also exhibited an inhibition of ~ 28 mm and ~ 33 mm against *S. aureus* and *E. coli*, respectively (**Figure S3**). The impregnation of PCL into the BC matrix is expected to impart flexibility in the prepared drug-loaded films, which when used as a wound dressing material will possess the ability to adapt to any shape of the wound.^{2,10} Also, the biocompatible nature of PCL will help in controlling the drug release for treating the local infections caused due to severe injuries. Generally, infection at the site of injuries is due to the presence of microorganisms and the effectiveness of the gentamicin- and streptomycin-loaded membranes showed promising results by inhibiting the cell multiplication with the release of the loaded drugs.

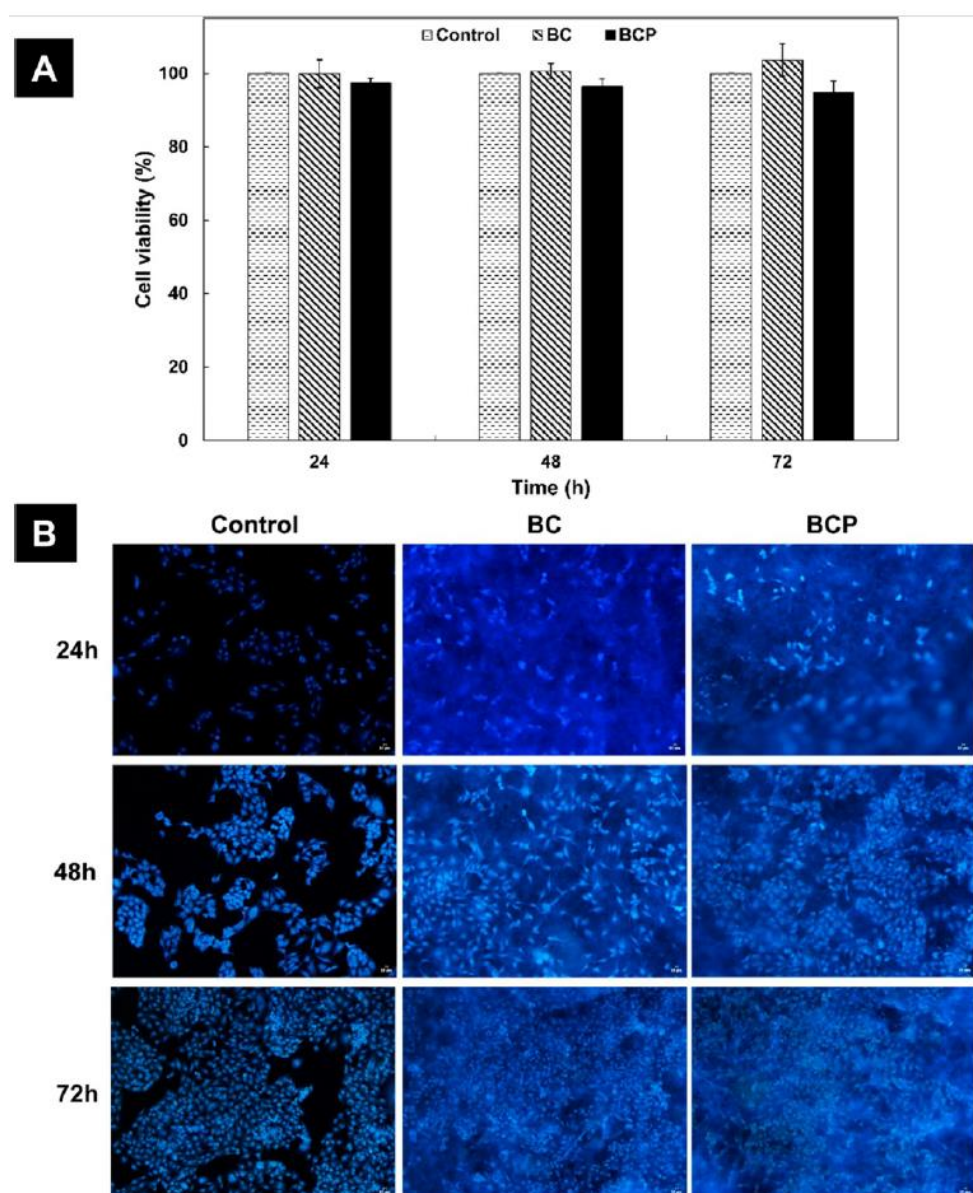


Figure 7. (A) Cell viability (%) of baby hamster kidney cells in contact with BC and BCP membranes incubated for 24 h, 48 h, and 72 h. (B) BHK-21 cell proliferation on the BC and BCP surfaces, after 24 h, 48 h, and 72 h of incubation, stained with DAPI.

The elemental composition of BC and drug-loaded BC membranes, BC-GEN and BC-SM was studied using EDX and represented in **Figure 6A**. Pure BC membrane comprises carbon (*C*) and oxygen (*O*) level of around 51% and 48%, respectively, in terms of weight percentage. However, the surface modification of BC with gentamicin sulfate and streptomycin sulfate resulted in an increase in nitrogen (*N*) level, thereby increasing the overall *C* + *N* along with the presence of sulfur (*S*), confirming the functionalization of BC membrane with GEN and SM (**Figure 6A**).²¹ The presence of *N* could be justified due to the presence of amine groups in both the aminoglycosidic antibiotics.⁴² As the drug solutions prepared were of very low concentration (0.2 and 0.5 mg/mL), the elemental composition did not reveal a higher percentage of sulfur.

However, even that amount of drug loading was sufficient to inhibit the bacterial growth as shown in the antimicrobial assay (**Figure 5A**). The structural and chemical composition of the fabricated drug-loaded scaffolds was studied by FT-IR spectroscopy (**Figures 6B,C**). The characteristic O—H and C—O—C stretching vibration bands present in BC are observed in the gentamicin- and streptomycin-loaded BC membranes (BG and BS, respectively) as shown in **Figure 6B**. Similarly, in **Figure 6C**, characteristic carbonyl and symmetric-asymmetric CH₂ stretching related to BCP are predominantly observed in both gentamicin- and streptomycin-loaded BCP membranes (BCG and BCS, respectively). The typical absorption bands corresponding to amide I, II, and III linkages are respectively observed at 1638, 1531, and 1261 cm⁻¹ in the BG sample and 1646, 1544, and 1235 cm⁻¹ in the BS sample, in **Figure 6B**.^{43,44} A slight shift and overlapping of the peaks have appeared due to inter and intramolecular hydrogen bonding, confirming the efficient encapsulation of the BCP membranes with gentamicin and streptomycin.

3.3. *In Vitro* Cytotoxicity

The prepared BC and BCP membranes were subjected to cytotoxicity test against baby hamster kidney cells to understand their biocompatible behavior. **Figure 7A** illustrates the cell attachment ability of the pure BC and developed BCP membranes. Pure BC had no cytotoxicity against BHK-21 cells and exhibited an excellent cell viability (~ 103%). This could be due to the presence of abundant hydroxyl groups in the BC structure, which benefitted the cell growth and adhesion.⁴⁵ Generally, BC is noncytotoxic in nature; however, the impregnation of usually biocompatible PCL into the BC matrix was carried out in this work to understand the overall biocompatibility of the prepared composite membrane (BCP) for biomedical application. As shown in **Figure 7A**, BCP membrane extract also showed no toxicity against the BHK-21 cells and exhibited 94% viability after 72 h. To use these membranes for long-term application, the cells were treated with the BC and BCP extracts for 24 h, 48 h, and 72 h, and it was observed that the extracts were nontoxic to the cells even after the long incubation period. Also from **Figure 7B**, it was clearly observed that the DAPI stained nuclei of the cells showed cell adhesion and proliferation on the BC and BCP surfaces, indicating their intact nature. Therefore, these results indicate that the fabricated BCP membranes exhibited biocompatibility toward baby hamster kidney cells and thus could be utilized as wound dressing material for infectious wounds.

3.4. *In Vitro* Drug Release and Kinetics

As observed from **Figure 6D**, both streptomycin and gentamicin exhibited burst release effect at around 6 h with the release of 23% of SM and 16% of GEN, respectively, into the phosphate buffered saline system. The rest of the streptomycin and gentamicin were slowly diffused to the system, and

~58% and ~42% of the drugs were released into the system after 48 h. The drug release profiles indicate a uniformly distributed BCP scaffold, which could be utilized as a wound dressing material.

4. CONCLUSIONS

The current research elucidates the BC and BCP based antimicrobial scaffolds produced by their functionalization with GEN and SM antibiotics. PCL has been used as a biomaterial in wound healing and other biomedical applications due to its flexibility, biocompatibility, and chemical stability. Therefore, the BC membranes were first impregnated with PCL, and the FTIR, SEM, and TGA analyses confirmed the interaction between BC and PCL resulting in the formation of flexible cellulose membranes. These membranes were then functionalized with the antibiotics, GEN and SM, and the resultant membranes exhibited excellent antimicrobial properties against model bacteria, *E. coli* and *S. aureus*. The fabricated BC and BCP composite membranes were biocompatible and nontoxic to BHK-21 cells even after 72 h, allowing cell proliferation. Thus, these results suggest that the GEN and SM functionalized BC and BCP membranes are ready to be utilized as an effective dressing material in future.

REFERENCES

- (1) Aydogdu, M. O.; Altun, E.; Ahmed, J.; Gunduz, O.; Edirisinghe, M. Fiber Forming Capability of Binary and Ternary Compositions in the Polymer System: Bacterial Cellulose-Polycaprolactone-Polylactic Acid. *Polymers (Basel)* **2019**, *11* (7), 1148.
- (2) Liu, W.; Du, H.; Zhang, M.; Liu, K.; Liu, H.; Xie, H.; Zhang, X.; Si, C. Bacterial Cellulose-Based Composite Scaffolds for Biomedical Applications: A Review. *ACS Sustain. Chem. Eng.* **2020**, *8* (20), 7536—7562.
- (3) Costa, A. F. S.; Almeida, F. C. G.; Vinhas, G. M.; Sarubbo, L. A. Production of Bacterial Cellulose by *Gluconacetobacter Hansenii* Using Corn Steep Liquor as Nutrient Sources. *Front. Microbiol.* **2017**, *8* (OCT), 1—12.
- (4) Czaja, W.; Krystynowicz, A.; Bielecki, S.; Brown, R. M. Microbial Cellulose - The Natural Power to Heal Wounds. *Biomaterials* **2006**, *27* (2), 145—151.
- (5) Pandit, A.; Kumar, R. A Review on Production, Characterization and Application of Bacterial Cellulose and Its Biocomposites. *J. Polym. Environ.* **2021**, *29*, 2738.
- (6) Choi, C. N.; Song, H. J.; Kim, M. J.; Chang, M. H.; Kim, S. J. Properties of Bacterial Cellulose Produced in a Pilot-Scale Spherical Type Bubble Column Bioreactor. *Korean J. Chem. Eng.* **2009**, *26* (1), 136—140.
- (7) Kaewnopparat, S.; Sansernluk, K.; Faroongsarng, D. Behavior of Freezable Bound Water in the Bacterial Cellulose Produced by *Acetobacter Xylinum*: An Approach Using Thermoporosimetry. *AAPS PharmSciTech* **2008**, *9* (2), 701—707.
- (8) Ul-Islam, M.; Khan, T.; Park, J. K. Water Holding and Release Properties of Bacterial Cellulose Obtained by in Situ and Ex Situ Modification. *Carbohydr. Polym.* **2012**, *88* (2), 596-603.

- (9) Wahid, F.; Zhao, X.; Zhao, X.; Ma, X.; Xue, N.; Liu, X.; Wang, F. ; Jia, S.; Zhong, C. Fabrication of Bacterial Cellulose-Based Dressings for Promoting Infected Wound Healing. *ACS Appl. Mater. Interfaces* **2021**, 13 (28), 32716 DOI: [10.1021/acscami.1c06986](https://doi.org/10.1021/acscami.1c06986).
- (10) Yang, G.; Xie, J.; Hong, F.; Cao, Z.; Yang, X. Antimicrobial Activity of Silver Nanoparticle Impregnated Bacterial Cellulose Membrane: Effect of Fermentation Carbon Sources of Bacterial Cellulose. *Carbohydr. Polym.* **2012**, 87 (1), 839-845.
- (11) Amin, M. C. I. M.; Abadi, A. G.; Ahmad, N.; Katas, H.; Jamal, J. A. Bacterial Cellulose Film Coating as Drug Delivery System: Physicochemical, Thermal and Drug Release Properties. *Sains Malaysiana* **2012**, 41 (5), 561-568.
- (12) Eslahi, N.; Mahmoodi, A.; Mahmoudi, N.; Zandi, N.; Simchi, A. Processing and Properties of Nanofibrous Bacterial Cellulose-Containing Polymer Composites: A Review of Recent Advances for Biomedical Applications. *Polym. Rev.* **2020**, 60 (1), 144-170.
- (13) Nair, L. S.; Laurencin, C. T. Biodegradable Polymers as Biomaterials. *Prog. Polym. Sci.* **2007**, 32 (8-9), 762-798.
- (14) Prasad, A.; Kandasubramanian, B. Fused Deposition Processing Polycaprolactone of Composites for Biomedical Applications. *Polym. Technol. Mater.* **2019**, 58 (13), 1365-1398.
- (15) Yamamoto, M.; Ikada, Y.; Tabata, Y. Controlled Release of Growth Factors Based on Biodegradation of Gelatin Hydrogel. *J. Biomater. Sci. Polym. Ed.* **2001**, 12 (1), 77-88.
- (16) Figueiredo, A. R. P.; Silvestre, A. J. D.; Neto, C. P.; Freire, C. S. R. In Situ Synthesis of Bacterial Cellulose/Polycaprolactone Blends for Hot Pressing Nanocomposite Films Production. *Carbohydr. Polym.* **2015**, 132, 400-408.
- (17) Muwaffak, Z.; Goyanes, A.; Clark, V.; Basit, A. W.; Hilton, S. T.; Gaisford, S. Patient-Specific 3D Scanned and 3D Printed Antimicrobial Polycaprolactone Wound Dressings. *Int. J. Pharm.* **2017**, 527 (1-2), 161-170.
- (18) Bayoumi, A.; Sarg, M. T.; Fahmy, T. Y. A.; Mohamed, N. F.; El-Zawawy, W. K. The Behavior of Natural Biomass Materials as Drug Carriers in Releasing Loaded Gentamicin Sulphate. *Arab. J. Chem.* **2020**, 13 (12), 8920-8934.
- (19) Elizondo, E.; Sala, S.; Imbuluzqueta, E.; González, D.; Blanco-Prieto, M. J.; Gamazo, C.; Ventosa, N.; Veciana, J. High Loading of Gentamicin in Bioadhesive PVM/MA Nanostructured Microparticles Using Compressed Carbon-Dioxide. *Pharm. Res.* **2011**, 28 (2), 309321.
- (20) Imbuluzqueta, E.; Elizondo, E.; Gamazo, C.; Moreno-Calvo, E.; Veciana, J.; Ventosa, N.; Blanco-Prieto, M. J. Novel Bioactive Hydrophobic Gentamicin Carriers for the Treatment of Intracellular Bacterial Infections. *Acta Biomater.* **2011**, 7 (4), 1599-1608.
- (21) Rouabhia, M.; Asselin, J.; Tazi, N.; Messaddeq, Y.; Levinson, D.; Zhang, Z. Production of Biocompatible and Antimicrobial Bacterial Cellulose Polymers Functionalized by RGDC Grafting Groups and Gentamicin. *ACS Appl. Mater. Interfaces* **2014**, 6 (3), 1439-1446.
- (22) Sharma, T.; Kumar, A.; Shah, S. S.; Bamezai, R. K. Analysis of Interactions between Streptomycin Sulphate and Aqueous Food Acids (L-Ascorbic Acid and Citric Acid): Physico-Chemical and Spectroscopic Insights. *J. Chem. Thermodyn.* **2020**, 151, 106207.

- (23) Sharma, S.; Kumar, K.; Chauhan, S.; Chauhan, M. S. Conductometric and Spectrophotometric Studies of Self-Aggregation Behavior of Streptomycin Sulphate in Aqueous Solution: Effect of Electrolytes. *J. Mol. Liq.* **2020**, 297, 111782.
- (24) Singh, M.; Schiavone, N.; Papucci, L.; Maan, P.; Kaur, J.; Singh, G. ; Nandi, U.; Nosi, D.; Tani, A.; Khuller, G. K.; Priya, M.; Singh, R.; Kaur, I. P. Streptomycin Sulphate Loaded Solid Lipid Nanoparticles Show Enhanced Uptake in Macrophage, Lower MIC in Mycobacterium and Improved Oral Bioavailability. *Eur. J. Pharm. Biopharm.* **2021**, 160, 100-124.
- (25) Bhagabati, P.; Hazarika, D.; Katiyar, V. Tailor-Made UltraCrystalline, High Molecular Weight Poly(ϵ -Caprolactone) Films with Improved Oxygen Gas Barrier and Optical Properties: A Facile and Scalable Approach. *Int. J. Biol. Macromol.* **2019**, 124, 1040-1052.
- (26) Bandyopadhyay, S.; Saha, N.; Saha, P. Characterization of Bacterial Cellulose Produced Using Media Containing Waste Apple Juice. *Appl. Biochem. Microbiol.* **2018**, 54 (6), 649-657.
- (27) Barud, H. S.; Ribeiro, S. J. L.; Carone, C. L. P.; Ligabue, R.; Einloft, S.; Queiroz, P. V. S.; Borges, A. P. B.; Jahno, V. D. Optically Transparent Membrane Based on Bacterial Cellulose/ Polycaprolactone. *Polimeros* **2013**, 23 (1), 135-138.
- (28) Jia, Y.; Wang, X.; Huo, M.; Zhai, X.; Li, F.; Zhong, C. Preparation and Characterization of a Novel Bacterial Cellulose/ Chitosan Bio-Hydrogel. *Nanomater. Nanotechnol.* **2017**, 7, 1-8.
- (29) Shao, W.; Wu, J.; Liu, H.; Ye, S.; Jiang, L.; Liu, X. Novel Bioactive Surface Functionalization of Bacterial Cellulose Membrane. *Carbohydr. Polym.* **2017**, 178 (June), 270-276.
- (30) Lin, W. C.; Lien, C. C.; Yeh, H. J.; Yu, C. M.; Hsu, S. H. Bacterial Cellulose and Bacterial Cellulose-Chitosan Membranes for Wound Dressing Applications. *Carbohydr. Polym.* **2013**, 94 (1), 603611.
- (31) Kotcharat, P.; Chuysinuan, P.; Thanyacharoen, T.; Techasakul, S.; Ummartyotin, S. Development of Bacterial Cellulose and Polycaprolactone (PCL) Based Composite for Medical Material. *Sustain. Chem. Pharm.* **2021**, 20, 100404.
- (32) Meza-Contreras, J. C.; Manriquez-Gonzalez, R.; Gutiérrez-Ortega, J. A.; Gonzalez-Garcia, Y. XRD and Solid State ^{13}C -NMR Evaluation of the Crystallinity Enhancement of ^{13}C -Labeled Bacterial Cellulose Biosynthesized by *Komagataeibacter Xylinus* under Different Stimuli: A Comparative Strategy of Analyses. *Carbohydr. Res.* **2018**, 461, 51-59.
- (33) Wang, M.; Li, J.; Shi, G.; Liu, G.; Muller, A. J.; Wang, D. Suppression of the Self-Nucleation Effect of Semicrystalline Polymers by Confinement. *Macromolecules* **2021**, 54 (8), 3810-3821.
- (34) Pinto, S. C.; Goncalves, G.; Sandoval, S.; López-Periago, A. M.; Borrás, A.; Domingo, C.; Tobias, G.; Duarte, I.; Vicente, R.; Marques, P. A. A. P. Bacterial Cellulose/Graphene Oxide Aerogels with Enhanced Dimensional and Thermal Stability. *Carbohydr. Polym.* **2020**, 230, 115598.
- (35) Wang, X.; Tang, J.; Huang, J.; Hui, M. Production and Characterization of Bacterial Cellulose Membranes with Hyaluronic Acid and Silk Sericin. *Colloids Surfaces B Biointerfaces* **2020**, 195 (July), 111273.
- (36) Oliveira, R. L.; Vieira, J. G.; Barud, H. S.; Assuncao, R. M. N.; Filho, G. R.; Ribeiro, S. J. L.; Messadeqq, Y. Synthesis and Characterization of Methylcellulose Produced from Bacterial Cellulose under Heterogeneous Condition. *J. Braz. Chem. Soc.* **2015**, 26 (9), 1861-1870.

- (37) Surma-Slusarska, B.; Presler, S.; Danielewicz, D. Characteristics of Bacterial Cellulose Obtained from *Acetobacter Xylinum* Culture for Application in Papermaking. *Fibres Text. East. Eur.* **2008**, 16 (4), 108-111.
- (38) Frone, A. N.; Panaitescu, D. M.; Chiulan, I.; Nicolae, C. A.; Casarica, A.; Gabor, A. R.; Trusca, R.; Damian, C. M.; Purcar, V.; Alexandrescu, E.; Stanescu, P. O. Surface Treatment of Bacterial Cellulose in Mild, Eco-Friendly Conditions. *Coatings* **2018**, 8 (6), 221.
- (39) Chiaoprakobkij, N.; Suwanmajo, T.; Sanchavanakit, N. Curcumin-Loaded Bacterial Cellulose/Alginate/Gelatin as A Multifunctional Biopolymer Composite Film. *Mol. Imprinted Sensors* **2020**, 25, 3800.
- (40) Milosevic, M.; Stojanovic, D. B.; Simic, V.; Grkovic, M.; Bjelovic, M.; Uskokovic, P. S.; Kojic, M. Preparation and Modeling of Three-layered PCL/PLGA/PCL Fibrous Scaffolds for Prolonged Drug Release. *Sci. Rep.* **2020**, 10 (1), 1-12.
- (41) Sunde, M.; Norstrom, M. The Genetic Background for Streptomycin Resistance in *Escherichia Coli* Influences the Distribution of MICs. *J. Antimicrob. Chemother.* **2005**, 56 (1), 87-90.
- (42) Castro, C.; Zuluaga, R.; Alvarez, C.; Putaux, J. L.; Caro, G.; Rojas, O. J.; Mondragon, I.; Ganán, P. Bacterial Cellulose Produced by a New Acid-Resistant Strain of *Gluconacetobacter* Genus. *Carbohydr. Polym.* **2012**, 89 (4), 1033-1037.
- (43) Dwivedi, C.; Pandey, H.; Pandey, A.; Ramteke, P. Fabrication and Assessment of Gentamicin Loaded Electrospun Nanofibrous Scaffolds as a Quick Wound Healing Dressing Material. *Curr. Nanosci.* **2015**, 11 (2), 222-228.
- (44) Unnithan, A. R.; Gnanasekaran, G.; Sathishkumar, Y.; Lee, Y. S.; Kim, C. S. Electrospun Antibacterial Polyurethane-Cellulose Acetate-Zein Composite Mats for Wound Dressing. *Carbohydr. Polym.* **2014**, 102 (1), 884-892.
- (45) Sun, B.; Wei, F.; Li, W.; Xu, X.; Zhang, H.; Liu, M.; Lin, J.; Ma, B.; Chen, C.; Sun, D. Macroporous Bacterial Cellulose Grafted by Oligopeptides Induces Biomimetic Mineralization via Interfacial Wettability. *Colloids Surfaces B Biointerfaces* **2019**, 183, 110457.